Analysis and Behavioral Modeling of TiO_2-based Resistance Switching Device

Gang Liu[1, a], Liang Fang[2,b]

[1]School of Computer, National University of Defense Technology, Changsha, Hunan 410073, China

[2]School of Computer, National University of Defense Technology, Changsha, Hunan 410073, China

[a] 38672251@qq.com, [b] lfang_cs@163.com

Keywords: Resistive random access memory (RRAM), Au/TiO_2/Au, Behavioral modeling.

Abstract. This paper presents a new behavioral model for TiO_2 resistive random access memory (RRAM). The model is based on hierarchical transformation filament theory, the device parameters are obtained from an Au/TiO_2/Au MIM (Metal/Insulator/Metal) RRAM cell with 100 nm in diameter, 50 nm-thick TiO_2 thin film. The proposed model can be applied to efficient simulation of large-scale RRAM array.

Introduction

Two-terminal Metal-insulator-Metal (MIM) architecture RRAM, with its good compatibility with the CMOS process, fast access speed, high reliability, and multi-level capability, has been considered as one of the most promising candidates for next generation nonvolatile memory [1, 2]. The resistance switching (RS) of an RRAM cell can be conducted by external bias voltage. High resistance state (HRS) and low resistance state (LRS) are used to encode either logic 0 or 1. RS phenomena have been found in many materials, especially in binary transition metal oxide [3]. Among these, TiO_2 thin film as a typical one, has gained much attentions [4, 6].

In this paper, a SPICE model of TiO_2 RS device is developed based on transformation filament theory. The developed model can easily be invoked in HSPICE simulation with accuracy and efficiency.

Analysis Of Mechanism

Generally, the effect of RS can be attributed to the formation and rupture of internal conductive filament (CF), which are considered caused by the composition impact of electrochemical and thermochemical [2, 3, 5, 7]. Recent researches discovered that the TiO2-x (x is oxygen sub-stoichiometry) or so-called Magnéli phase can be regarded as the dominant type of CF in rutile TiO2. With the electric-field-driven phenomenon, the oxygen vacancies are generated at anodic electrode, this procedure can be described by Kroger–Vink nomenclature [5] as follows:

$$O_O^X \rightarrow V_O^{"} + 2e^- + \frac{1}{2}O_2 . \quad (1)$$

Oxygen vacancies and electrons will drift with the driving force of electric-field, and the electrons can be captured by neighboring Ti ions：

$$Ti^{4+} + me^- \rightarrow Ti^{(4-m)+} . \quad (2)$$

In the process of electroforming, oxygen sub-stoichiometry (x) of oxygen-deficient TiO_x changes gradually in the interface of Metal/TiO_2 [7], in other words, the length of CF grows. The CF can be regarded as a hierarchical structure. The CF, which also can be described as Ti_nO_{2n-1} becomes weaker

in deeper layers, that is to say the 'n' number in the Ti_nO_{2n-1} is increasing. Generally, with the Magnéli phase becomes weaker, CF conductivity is descending. With the increasing of electric field, CF connects two electrodes when the bias voltage exceeds the threshold voltage (V_{set}). The conductivity jumps sharply, device is switched into LRS (SET procedure). One thing should be noticed is that the threshold voltage is time dependent, it changes with voltage sweep rate [10, 11]. This should be considered in application-oriented design. In LRS, bottom electrode is grounded, when negative bias voltage is applied to top electrode, CF will be ruptured if bias voltage exceeds the threshold voltage (V_{reset}), device is switched to HRS (RESET procedure). In LRS, electric field driven migration of oxygen vacancies can be neglected because of the high conductivity, so Joule heating may be the predominant issue in RESET.

Fabrication and Measurement

The fabrication of device was based on out previous work [8]: the 200 nm thick Au thin film bottom electrode was fabricated by electron-beam evaporation on a SiO_2/p-type-silicon substrate, and then a lift-off photolithographic process was followed. The 50 nm thick TiO_2 film was fabricated by reactive sputtering, and Au top electrode was also fabricated by electron beam evaporation and followed by lift-off photolithographic process.

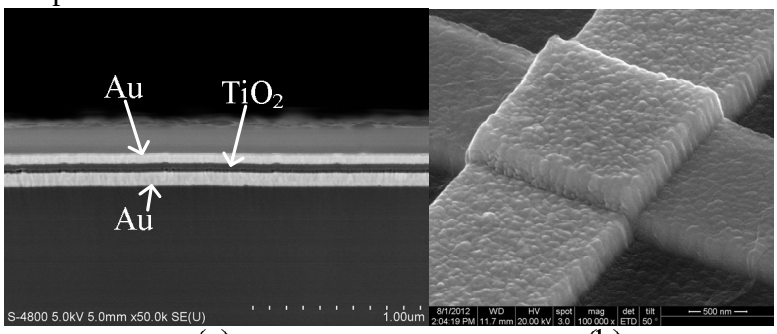

Fig. 2. $Au/TiO_2/Au$ device SEM imagine after lift-off photolithographic process. (a) Section and (b) Single cell.

I-V characteristics of the device were measured by Agilent B1500A Semiconductor Characterization System in room temperature. According to the previous analysis, 4 steps of CF transformation are depicted In Fig. 3.

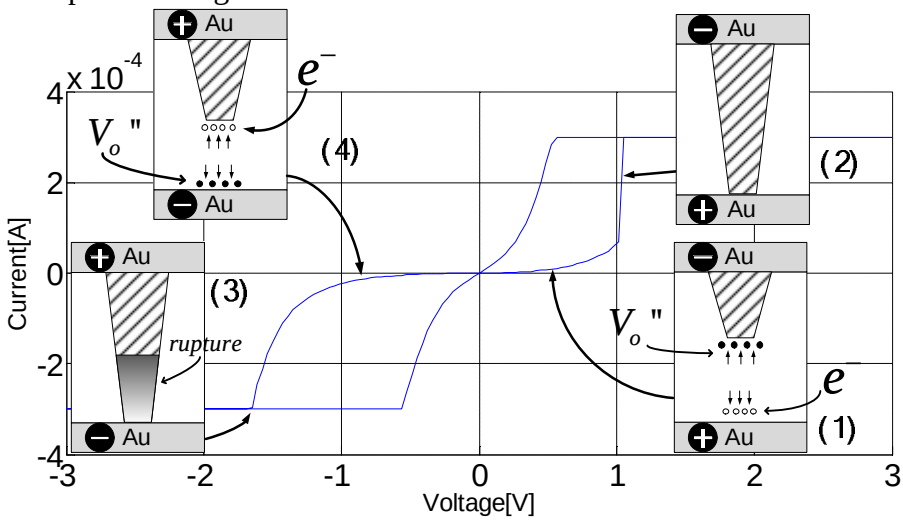

Fig. 3. I-V characteristics of $Au/TiO_2/Au$ device. Current compliance was set to 0.3 mA. The insets shows different stages of switching procedure.

In inset (1), with electric field and Joule heating effect, electrons and oxygen vacancies are generated and migrate in opposite directions. CF grows from cathode interface. Inset (2), when the bias voltage reaching the voltage V_{set}, CF connects two electrodes, the device is switched to LRS state. Inset (3), CF is ruptured due to Joule heating and the electric field. Inset (4), after CF ruptured, the device is switched to HRS state again. It is necessary to emphasize that the I-V characteristics in LRS is not a perfect linear, this may due to bulk-assisted re-oxidation, which may occur in the filament tip.

Device Model

The behavioral model is based on analysis which were discussed earlier, and the model parameters are obtained from Au/TiO_2/Au device experimental data.

Model Parameter. Device in HRS and LRS can be described using previous analyzed hierarchical transformation mechanism. An exponential relation is chosen to account for the nonlinear electric conductivity of a generalized filament [9].

$$\sigma_{disc} = \sigma_{disc,0} \cdot \exp(\frac{V_{bias}}{V_0}) . \quad (1)$$

Where σ_{disc} is the filament electric conductivity, V_{bias} is the bias voltage, $\sigma_{disc,0}$ and V_0 are constants. From Eq. 1 and typical resistor equation, the relation of current and voltage can be obtained:

$$I = \frac{V_{bias} \cdot \sigma_{disc,0} \cdot \exp(\frac{|V_{bias}|}{V_0}) \cdot s}{l} . \quad (2)$$

Where s and l are CF section area and length respectively, l is set to 40 nm for HRS cell. Other setting as follows: In HRS, s = 100 nm^2, V_0 = 0.454 V, $\sigma_{disc,0} = 2\times10^3$ S/m; in LRS, $\sigma_{disc,0} = 6\times10^4$ S/m, V_0 = 0.456 V. According to previous research, the V_{set} cannot be regarded as a fixed value, it varies with voltage sweep rates. In [10], the relation of V_{set} and voltage sweep rate can be evaluated as

$$V_{set} = V_1 \cdot \log(\frac{\beta \cdot \tau_0}{V_1}) . \quad (3)$$

Where V_1 and τ_0 are constants, β is the sweep rate. According to experimental data, V_{set} is set to 1.013 V, β is set to 0.4 V/s, this can be obtained by assuming V_1= 0.03 V, τ_0=3.4653×1013 s.

RRAM cell Simulation. According to Eq. 2, the behavioral model was built by Verilog-A, and simulations were implemented by HSPICE. I-V characteristics comparison of proposed model and experimental data were shown in Fig. 4(a), compliance current was set to 0.3mA. Transient simulations of SET and RESET operation and corresponding current were shown in Fig. 4(b)

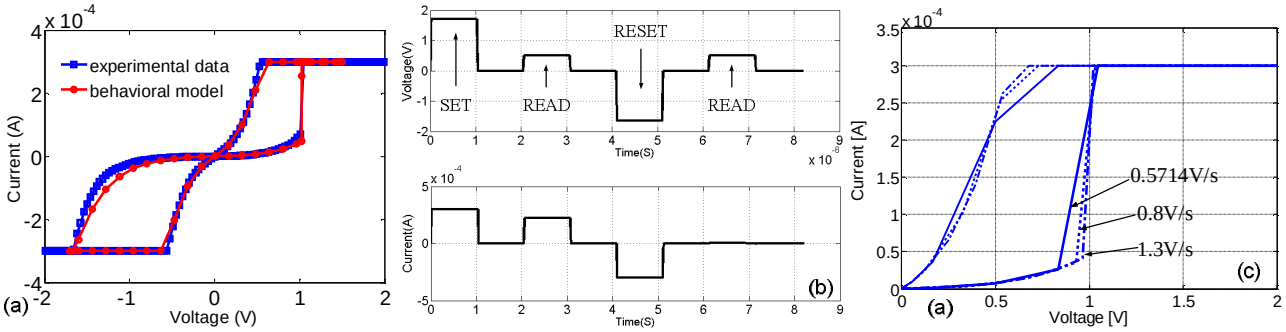

Fig. 4. Simulation curves of (a) I-V characteristicd, (b) transient analysis and (c) Vset drift with various sweep rates.

Fig. 4(a) shows the I-V characteristics of behavioral model are in good agreement with experimental data. SET and RESET pulses were applied to behavioral model alternately, and each pulse followed by a verify read pulse, as shown in Fig. 4(b), the model can effectively switched between LRS and HRS. In Fig.4(c), V_{set} increasing with the growth of sweep rate, according to Eq. 3, it has an upper limitation which depends on electric field.

Conclusion. In this paper, we present a behavioral model of TiO_2 resistance switching device. This model is based on analysis of physical mechanism, and it can capture the characteristic of the device well. Simulations were implemented by HSPICE, the model proposed can be applied in large-scale RRAM design.

Acknowledgements

This work was supported by the National Natural Science Foundation of China (Grant No. 61332003).

References

[1] Beck, J. G. Bednorz, C. Gerber, C. Rossel, and D.Widmer, "Reproducible switching effect in thin oxide films for memory applications," IEEE Electron Device Lett., vol. 77, no. 1, 2000, pp. 139–141.
[2] Hiroyuki Akinaga and Hisashi Shima. Resistive Random Access Memory (ReRAM) Based on Metal Oxides. Proc. IEEE, vol. 98, no. 12, pp. 2237-2251. 2010.
[3] Carsten Kügeler, Roland Rosezin, Eike Linn, Rainer Bruchhaus, Rainer Waser. Materials, technologies, and circuit concepts for nanocrossbar-based bipolar RRAM. Appl Phys A (2011) 102: 791-809.
[4] Choi, B. J. et al. Resistive switching mechanism of TiO_2 thin films grown by atomic-layer-deposition. J. Appl. Phys. 98, 033715 (2005).
[5] Kyung Min Kim, Doo Seok Jeong, Cheol Seong Hwang. Nanofilamentary resistive switching in binary oxide system; a review on the present status and outlook. Nanotechnology, 22 (2011) 254002 (17pp).
[6] Doo Seok Jeong, Herbert Schroeder, Uwe Breuer, and Rainer Waser. Characteristic electroforming behavior in Pt/TiO_2/Pt resistive switching cells depending on atmosphere. J. Appl. Phys. 104, 123716 (2008).
[7] K Szot, M Rogala, R Waser et al. TiO2—a prototypical memristive material. Nanotechnology, 22, (2011), 254001, (21pp).
[8] Yan A, Liu G, Zhang C, et al. The Study of Au/TiO_2/Au Resistive Switching Memory with Crosspoint Structure[J]. Advanced Materials Research, 2013, 654:659-663.
[9] Stephan Menzel, Matthias Waters, Rainer Waser et al. Origin of the Ultra-nonlinear Switching Kinetics in Oxide-Based Resistive Switches. Adv. Funct. Mater. 2011, 21, 4487-4492.
[10] Carlo Cagli, Federico Nardi, and Daniele Ielmini. Modeling of Set/Reset Operations in NiO-Based Resistive-Switching Memory Devices. IEEE TRANSACTIONS ON ELECTRON DEVICES, VOL. 56, NO. 8, AUGUST 2009.
[11] S. H. Jo, K.-H. Kim and W. Lu, Programmable resistance switching in nanoscale two-terminal devices, Nano Lett., 2009, 9, 496–500.